Proton Remains Puzzling

Haiyan Gao[1,2,*], Tianbo Liu[1,2,†], Chao Peng[1,‡], Zhihong Ye[3,§], and Zhiwen Zhao[1,¶]

[1] *Duke University, Durham, NC 27708, U.S.A.*

[2] *Duke Kunshan University, Kunshan, Jiangsu 215316, China*

[3] *Argonne National Laboratory, Argonne, IL 60439, U.S.A.*

Nucleons are building blocks of visible matter, and are responsible for more than 99% of the visible mass in the universe despite the fact that the discovery of the Higgs boson is almost irrelevant to the origin of the proton mass. While major progress has been made in the last two decades in understanding the proton spin puzzle discovered in the late 1980s by the European Muon Collaboration, a new proton puzzle emerged in the last several years concerning the proton charge radius, which is the charge weighted size of the proton. In this paper we will review the latest situation concerning the proton charge radius, mass and spin, and discuss upcoming new experiments addressing these puzzles, as well as implications for new physics.

1 Introduction

Nucleons are known as the fundamental building blocks of the visible matter. In 1933, Otto Stern discovered that the magnetic moment of the proton disagreed with Dirac's prediction $\mu = e\hbar/2M$ for a structureless spin-1/2 particle. This discovery for the first time indicated that the proton is not a pointlike particle, rather it has internal structure. In 1950s, the electron-proton elastic scattering experiments by Hofstadter and others at Stanford University uncovered the spatial charge and current distributions of the nucleon. A decade later, the experimental efforts in deep-inelastic scattering (DIS) of electrons on protons pioneered by Friedman, Kendall and Taylor at the Stanford Linear Accelerator Center (SLAC) revealed the point-like constituent particles inside the proton, and led to the establishment of the quark model and the experimental foundation for the development of Quantum Chromodynamics (QCD).

QCD, a theory with quarks and gluons as the underlying degrees of freedom is the accepted theory of strong interaction. It has two important features: asymptotic freedom and confinement. While the former refers to the feature that the strong coupling constant becomes weaker and weaker as energies involved become higher and higher or the corresponding length scale becomes smaller and smaller, the latter refers to the fact that quarks do not exist in isolation but exist as colorless hadrons: mesons or baryons. While QCD has been extremely well tested at high energies by experiments where perturbative calculations can be carried out and be compared with, an analytical solution to the QCD Lagrangian in the nonperturbative region is notoriously difficult and out of reach. As such our knowledge about how QCD works in the confinement region, where the strong coupling constant is strong, is rather poor. Nucleons, building blocks of atomic nuclei, provide a natural and an effective laboratory for physicists to study QCD in the confinement region.

The structure of nucleons is a rich, exciting and vibrant research area, which involves studies of the ground state properties (mass, charge, spin, etc.) and distributions (charge, current, momentum, one-dimensional and three-dimensional parton distribution functions, etc.). Lepton scattering, particularly electron scattering, has been proven to be a powerful microscope in probing the nucleon structure. It is a clean probe with the advantage of higher-order contributions being suppressed. With the development in polarized beam, recoil polarimetry, and polarized target technologies, polarized experiments have provided more precise data on quantities ranging from electromagnetic form factors of the

*Email: gao@phy.duke.edu

†Email: liutb@jlab.org

‡Email: cp121@phy.duke.edu

§Email: yez@jlab.org

¶Email: zwzhao@jlab.org

nucleon [1, 2, 3] through elastic electron-nucleon scattering to spin structure functions [4] probed in deep-inelastic lepton-nucleon scattering. In this paper, we will discuss the latest status on the proton charge radius, proton mass, and proton spin, and upcoming new experiments. Further, we will discuss nucleon tomograph, particularly the transverse momentum dependent parton distribution functions (TMDs), and nucleon tensor charge and its connection to new physics through quark and neutron electric dipole moments.

2 Proton Radius Puzzle and PRad Experiment

The proton charge radius, a fundamental quantity describing the size of the proton weighted by its charge distribution, is important not only for QCD, but also for bound state QED calculations and ultrahigh precision tests of QED. As such both atomic physicists and nuclear physicists have been working on hydrogen spectroscopy and electron scattering experiments, respectively, for decades in order to determine this quantity precisely.

The absolute frequency of transitions between H energy levels can be measured with an accuracy of 1.4 part in 10^{14} via the comparison with an atomic cesium fountain clock as a primary frequency standard. Such a precise measurement with the state-of-the-art QED calculations that include corrections for the finite size of the proton can indirectly determine the proton charge radius. The precision of this method is significantly enhanced by measuring the Lamb shift of muonic hydrogen. The contribution from the proton finite size term to the Lamb shift is much larger in muonic hydrogen than that in atomic hydrogen due to the fact that the muon mass is about 206 times of the electron mass. Such measurement was achieved at PSI in 2010 [5], and its result was reinforced by the same group in 2013 [6], which reported that $r_p = 0.84087 \pm 0.00039\,\mathrm{fm}$. These measurements obtained the most precise value of the proton charge radius; its uncertainty was less than 0.05%.

The proton charge radius can be determined directly from the slope of the proton electric form factor G_E^p extracted from elastic ep scattering measurements down to a momentum transfer squared value (Q^2) near zero as

$$\sqrt{\langle r^2 \rangle} = \sqrt{-6 \frac{dG_E^p\,(Q^2)}{dQ^2}\bigg|_{Q^2=0}}\,. \qquad (1)$$

Thus, the G_E^p data at $Q^2 \to 0$ are essential for this method. However, all existing experiments using magnetic spectrometers were limited by the lowest values of Q^2 that they could reach, and therefore relied on extrapolations down to $Q^2 \to 0$.

The recent experiment at Mainz [7, 8] measured the cross sections of elastic ep scattering within $Q^2 = 0.003 - 1.0\,\mathrm{GeV}^2$. Three spectrometers were utilized to cover a large amount of overlapping data sets. The statistical uncertainties of the measured cross-sections are lower than 0.2%. Both the electric and magnetic form factors of the proton were extracted by fitting the cross-section data. The recoil proton polarization experiment at Jefferson Lab [9] measured the elastic form factor ratio $\mu_p G_E/G_M$ of proton for $Q^2 = 0.3 - 0.7\,\mathrm{GeV}^2$. They extracted the proton charge radius by fitting the global data at $Q^2 < 0.5\,\mathrm{GeV}^2$. The two experimental results are consistent with each other. However, they are $3 - 5\,\sigma$ larger than the PSI value. The recent re-analyses of world ep scattering data indicate the systematic uncertainties were underestimated in the previous results, but this underestimation cannot account for the discrepancy [10, 11].

The "proton radius puzzle" refers to this fact that the ultrahigh precise value of the proton charge radius determined from muonic hydrogen Lamb shift measurements is about 5.5σ smaller than the value of CODATA 2014 compilation [12], which is a weighted average of world data from hydrogen spectroscopic measurements and elastic electron-proton scattering experiments. In Fig. 1, we show the discrepancy between PSI values and other experimental or analysis results.

This puzzle motivated intensive revisit of the QED calculations of the muonic hydrogen Lamb shift, including the evaluation of the proton polarizability contribution [14, 15, 16], yet no terms that can account for this discrepancy were found. The refined calculations were summarized in [17, 18]. New physics that may explain the puzzle was also explored, such as new

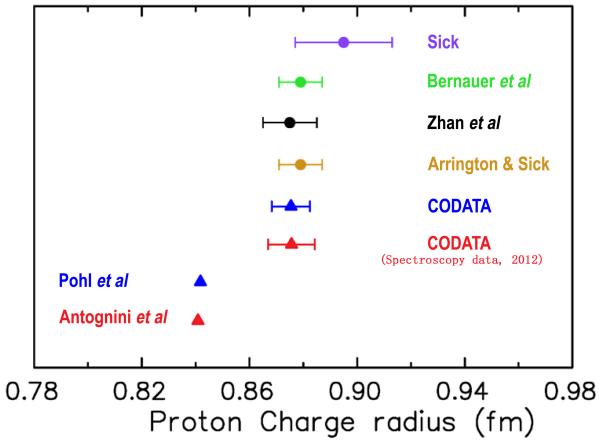

Fig. 1: A comparison between the proton charge radius from PSI, CODATA, as well as the elastic *ep* scattering measurements [9, 7, 8] and analyses [13, 10].

particles [19, 20], new parity violating muonic force [21], and quantum gravity at the Fermi scale [22]. In addition, some explanations in terms of the dispersion relations [23] or frame transformations [24, 25] were proposed to resolve the puzzle, but the former was inconsistent with [26], while the latter remained unconfirmed. After all, the understanding of the "proton radius puzzle" awaits for input from new dedicated experiments. Recent re-analyses of existing proton form factor data claimed the proton radius puzzle could be resolved by focusing on the low Q^2 part of the data [27, 28], but their truncation procedure was disagreed with that by the authors of [29].

To investigate the proton charge radius puzzle, a precise experiment based on the *ep* elastic scattering with totally different systematic uncertainties is necessary to check results from previous *ep* scattering experiments. Thus, the proton charge radius (PRad) experiment was approved with A rating by the Jefferson Lab Program Advisory Committee to take place in Hall B [30]. The PRad experiment aims to precisely determine the proton charge radius based on the cross-section measurement of the elastic *ep* scattering with a calorimetry method. As shown in Fig. 2, the experiment utilizes a high resolution, high efficiency calorimeter (HyCal) as the main detector. The calorimetric setup enables the experiment to reach the very forward angles and thus the very low Q^2 region $\left(\geq 2 \times 10^{-4}\,\mathrm{GeV}^2\right)$ that was never achieved before by magnetic spectrometer based measurements. As supplemental detectors, two GEM chambers at the upstream of HyCal can significantly increase the position resolution and reduce the systematic errors in the Q^2 determination. The hydrogen target used in PRad is a windowless gas-flow target. By removing the target windows, this experiment will not suffer from the typical background source of all previous *ep* experiments in order to reach the most forward scattering angles. The scattered electrons from the elastic *ep* scattering and Møller scattering will be simultaneously detected. The cross-sections of elastic *ep* scattering will hence be normalized to those of the Møller process, which can be precisely calculated in QED.

The extracted proton charge radius is expected to have a sub-percent precision. The systematic errors will be totally different from those in previous magnetic spectrometer based experiments. Its result will shed light on the discrepancy between the *ep* scattering experiments and the Lamb shift measurements of muonic hydrogen. Together with the μp elastic scattering experiment at PSI [31], the Initial State Radiation (ISR) experiment at Mainz [32], and new hydrogen spectroscopy experiments [33], these high precision experiments will have direct impacts and resolve the "proton radius puzzle". The PRad experiment is scheduled to take data in late spring of 2016.

3 Proton Mass

Mass, as the eigenvalue of the Hamiltonian, is the most fundamental property of a particle.

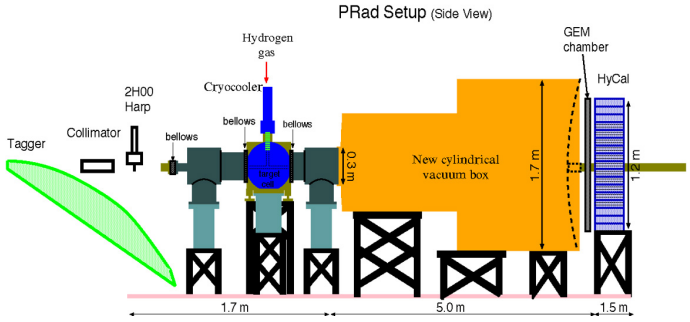

Fig. 2: The layout of the PRad experiment. It is not to scale.

With the discovery of the Higgs boson [34, 35] that provides the origin of the fermion mass, the standard model is complete. However, the current u and d quark mass, around several MeV, is less than one percent of that of the proton, which, together with the neutron, contributes more than 99% of the visible mass in the Universe. The vast mass is not from the Higgs boson but the dynamical chiral symmetry breaking (DSCB) [36], which is one of the most important features of nonperturbative QCD. Through the quantization of the classical QCD with massless quarks and gluons, a large mass scale is also generated [37]. Therefore, the understanding of the composition of the proton mass is a fundamental issue in nuclear and particle physics.

The proton, as the bound state of strong interaction, is fundamentally described in terms of quarks and gluons degrees of freedom in QCD. Thus, a partition of the proton mass can be investigated from QCD energy-momentum tensor,

$$\begin{aligned} T^{\mu\nu} &= \frac{1}{2}\bar{\psi} i D^{(\mu}\gamma^{\nu)}\psi - g^{\mu\nu}\bar{\psi}(i\not{D} - m)\psi \\ &\quad -F^{a\mu\rho}F^{a\nu}_{\ \ \rho} + \frac{1}{4}g^{\mu\nu}F^{a\rho\sigma}F^{a}_{\rho\sigma}. \end{aligned} \quad (2)$$

It defines the Hamiltonian operator of QCD,

$$H = \int d^3\mathbf{x} T^{00}(0,\mathbf{x}), \quad (3)$$

and the matrix element of the Hamiltonian in the rest frame gives the proton mass[1]. Following the procedure in Refs. [39, 40], the energy-momentum tensor can be uniquely separated into a traceless and a trace parts,

$$T^{\mu\nu} = \overline{T}^{\mu\nu} + \hat{T}^{\mu\nu}, \quad (4)$$

and each of them is scale independent. The corresponding matrix elements are

$$\langle P|\overline{T}^{\mu\nu}|P\rangle = \frac{1}{M}\left(P^\mu P^\nu - \frac{1}{4}g^{\mu\nu}M^2\right), \quad (5)$$

$$\langle P|\hat{T}^{\mu\nu}|P\rangle = \frac{1}{4}g^{\mu\nu}M, \quad (6)$$

where M is the proton mass. For a further separation, one may introduce two parameters a and b to respectively define the fractions of quark operator contribution to the traceless and the trace parts. Both a and b are scale dependent. According to the separation of the energy-momentum tensor, one has the partition of the Hamiltonian,

$$H = H_q + H_g + H_m + H_a, \quad (7)$$

where

$$H_q = \int d^3\mathbf{x}\psi^\dagger(-i\mathbf{D}\cdot\alpha)\psi, \quad (8)$$

$$H_g = \int d^3\mathbf{x}\frac{1}{2}(E^2 + B^2), \quad (9)$$

$$H_m = \int d^3\mathbf{x}\frac{1}{4}(1+\gamma_m)\bar{\psi}m\psi, \quad (10)$$

$$H_a = \int d^3\mathbf{x}\frac{1}{4}\beta(g)(E^2 - B^2). \quad (11)$$

$\beta(g)$ is the beta-function of QCD, and γ_m is the anomalous dimension of the mass operator and can be consistently neglected at leading order. Then, the matrix elements of each term are determined by the two parameters as

$$M_q = \frac{3}{4}\left(a - \frac{b}{1+\gamma_m}\right)M, \quad (12)$$

$$M_g = \frac{3}{4}(1-a)M, \quad (13)$$

$$M_m = \frac{4+\gamma_m}{4(1+\gamma_m)}bM, \quad (14)$$

$$M_a = \frac{1}{4}(1-b)M, \quad (15)$$

[1] A frame independent Hamiltonian can be defined in the front form with invariant mass square as the eigenvalue [38].

which are respectively interpreted as the contributions from quark energy, gluon energy, quark mass and trace anomaly.

The meaning of $a(\mu^2)$ is the momentum fraction carried by quarks in the infinite momentum frame,

$$a(\mu^2) = \sum_q \int_0^1 dx[f^q(x) + f^{\bar{q}}(x)], \qquad (16)$$

where μ is the scale. It can be obtained through the deep-inelastic lepton-proton scatterings and has been precisely measured. Its value from recent MMHT2014 [41] leading order parametrization is 0.546 ± 0.005 at $\mu = 2\,\mathrm{GeV}$.

The parameter $b(\mu^2)$ is related to the scalar charge of the proton as

$$b(\mu^2) = \langle P|m_u\bar{u}u + m_d\bar{d}d + m_s\bar{s}s|P\rangle/M, \quad (17)$$

where the contribution from heavy quarks has been neglected. The first two terms can be obtained from the pion-nucleon σ-term, which is defined as

$$\sigma_{\pi N} = \langle P|\hat{m}(\bar{u}u + \bar{d}d)|P\rangle, \qquad (18)$$

where $\hat{m} = (m_u + m_d)/2$ is the average of two light quark masses. A recent determination from high-precision data gives the value of the $\sigma_{\pi N}$ as $59.1 \pm 1.9 \pm 3.0\,\mathrm{MeV}$ [42]. Then, the main uncertainty comes from the scalar charge of the strange quark. A renormalization independent ratio

$$y = \frac{2\langle P|\bar{s}s|P\rangle}{\langle P|\bar{u}u + \bar{d}d|P\rangle} \qquad (19)$$

is usually defined to describe the strange content in the proton. Then, the strangeness σ-term can be expressed as

$$\sigma_{sN} = \langle P|m_s\bar{s}s|P\rangle = \frac{y}{2}\frac{m_s}{\hat{m}}\sigma_{\pi N}. \qquad (20)$$

In recent years, there are many lattice QCD calculations of the strange term [43, 44, 45, 46, 47, 48, 49, 50, 51, 52, 53, 54]. Besides, it is also suggested to constrain the strangeness content by measuring the ϕ-meson mass shift in nuclear matter [55]. In Fig. 3, we plot the proton mass budget, which is estimated at the scale $\mu = 2\,\mathrm{GeV}$ with the current quark mass ratio $m_s/\hat{m} = 27.5 \pm 1.0$ in Ref. [56], quark momentum fraction from MMHT2014 leading order parametrization [41], pion-nucleon σ-term determined in Ref. [42] and the most recent lattice calculation of strangeness content [54]. This partition is qualitatively in agreement with the estimation two decades ago [39]. Quantitatively, the contribution from quark mass, i.e. the explicit chiral symmetry breaking effect, is reduced, since the most recent determination of the strangeness content $y = 0.058(6)(8)$ from lattice QCD [54] is much smaller than the one, $y \sim 0.2$, adopted twenty years ago. The corresponding value of b parameter is 0.113 ± 0.010. We should also note that our estimation is at $2\,\mathrm{GeV}$ scale instead of $1\,\mathrm{GeV}$ scale in Ref. [39], as the global fit of the current quark mass in Ref. [56] is provided at $2\,\mathrm{GeV}$, but this effect on the determination of the b value is negligible.

To truly understand the proton mass budget, it is required to have precise constraint on the b parameter from experiments. With the knowledge of the a parameter which has been accurately extracted from DIS data, the determination of the b parameter will not only pin down quark energy term, but also more importantly provide direct access to the quark mass and the trace anomaly terms. In particular, the experimental access to the trace anomaly, which is an important quantum effect, may have profound influence on our understandings on nonperturbative QCD.

According to the definition of b parameter mentioned previously, it is determined by the scalar charge from u, d, and s quarks. Although the u and d quark terms have been precisely measured through the pion-nucleon σ-term, it is still challenging but important to measure the strangeness term, as the mass of strange quark is much larger than that of u and d quarks. This kind of measurement is recently proposed through the ϕ-meson mass shift in nuclear matter [55]. On the other hand, it is also possible to directly extract the parameter b via the purely real amplitude of the interaction between heavy quarkonium and light hadron at low energy [57, 58].

According to Ref. [57], the J/ψ-N scattering amplitude is expressed as

$$F_{J/\psi N} = r_0^3 d_2 \frac{2\pi^2}{27}(2M^2 - bM), \qquad (21)$$

where $r_0 = 4/(3\alpha_s m_c)$ is the "Bohr" radius and d_2 is the Wilson coefficient. The heavy quarkonium, such as J/ψ, is a strongly bound state

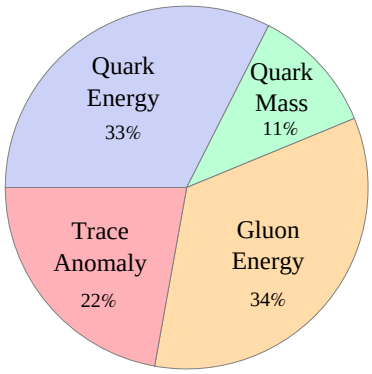

Fig. 3: Proton mass budget. It is estimated at the scale $\mu = 2\,\text{GeV}$ with quark momentum fraction 0.546 [41], $\sigma_{\pi N} = 59.1\,\text{MeV}$ [42] and $y = 0.058$ [55].

of two heavy quarks with both the constituent's mass and the binding energy much larger than $\Lambda_{\text{QCD}} \sim 340\,\text{MeV}$ [59], the typical nonperturbative QCD scale. Thus, it can be utilized as a microscopic probe to the structure of light hadrons, such as the proton. Although the quarkonium-nucleon scattering $J/\psi N \to J/\psi N$ is not directly accessible, the photoproduction process $\gamma N \to J/\psi N$ can be precisely measured with carefully designed experiments. They are related through the conventional vector meson dominance (VMD) approach for the differential cross-section of forward J/ψ-photoproduction on nucleons as [58]

$$\frac{d\sigma_{\gamma N\to J/\psi N}}{dt} = \frac{3\Gamma(J/\psi \to e^+e^-)}{\alpha m_{J/\psi}} \left(\frac{k_{J/\psi N}}{k_{\gamma N}}\right)^2 \frac{d\sigma_{J/\psi N\to J/\psi N}}{dt}, \tag{22}$$

where $k_{ab}^2 = [s-(m_a+m_b)^2][s-(m_a-m_b)^2]/4s$ denotes the momentum square of the reaction in centre-of-mass frame, and Γ stands for the partial J/ψ decay width. The differential cross-section of $J/\psi - N$ at low energy is expressed with the amplitude as

$$\frac{d\sigma_{J/\psi N\to J/\psi N}}{dt} = \frac{1}{64\pi}\frac{1}{m_{J/\psi}^2(\lambda^2 - m_N^2)} F_{J/\psi N}^2, \tag{23}$$

where $\lambda = (pK/m_{J/\psi})$ is the nucleon energy in the quarkonium rest frame, and p, K, and q are the four-momenta of the target nucleon, J/ψ and the initial photon, respectively. With this approach, one can extract the scattering amplitude $F_{J/\psi N}$ in (21), which can be utilized to determine the b parameter and furthermore the trace anomaly part of the proton mass.

Unfortunately, the existing data of the J/ψ-photoproduction near threshold are too sparse to precisely extract the real amplitude of the low-energy scattering [57, 58]. The near threshold electroproduction of J/ψ experiment is hence motivated. The SoLID spectrometer at Jefferson Lab is designed to operate in a high luminosity environment with large acceptance, and thus presents the unique advantage for such a measurement where the cross-section is small and rapidly changing. The exclusive J/ψ-electroproduction process will be measured in this experiment [60], and both the differential and total cross-sections of this reaction close to the threshold will be precisely extracted. The result will shed light on the determination of the b parameter and consequently the trace anomaly part of the proton mass. Besides, the multi-gluon exchange interaction between J/ψ and nucleon [61, 62] will also be examined in this experiment [60].

4 Proton Spin

4.1 Proton Spin Crisis and Angular Momentum Decomposition

In 1988, the European Muon Collaboration first measured quark helicity distribution in the proton through the polarized DIS processes [63, 64], and found that the quark spin only contributes a

small fraction to the proton spin. In recent analyses, the fraction is about 30% [65, 66, 67][2]. This result severely deviated from the naive quark model expectation that the proton spin is the sum of quark spins, and caused the "proton spin crisis". It has puzzled the physics society for more than 25 years.

Due to the Wigner rotation effect [68] which relates the spinors in different frames, the quark spin in proton rest frame will decompose into a spin part and an orbital angular momentum part in the infinite momentum frame (IMF) or the light-cone formalism where the parton language is well defined [69, 70]. Therefore, the measurement of quark orbital angular momentums plays an important role in understanding the proton spin puzzle, although the gluon also contributes a large fraction [71].

However, the decomposition of the proton spin into quark and gluon degrees of freedom is nontrivial, and it is still under debate [72, 73]. One well-known decomposition was proposed by Jaffe and Manohar [74]:

$$\begin{aligned} J_p &= \frac{1}{2}\Delta\Sigma + L_q + \Delta G + L_g \\ &= \frac{1}{2}\bar{\psi}\gamma^+\gamma_5\psi - i\bar{\psi}\gamma^+ r\times\nabla\psi + E\times A \\ &\quad + E\cdot(r\times\nabla)A. \end{aligned} \tag{24}$$

In this decomposition, the L_q as well as ΔG and L_g is not obviously gauge-invariant and thus lacks clear physical meanings. To solve this problem, a manifestly gauge-invariant decomposition was proposed by Ji [75]:

$$\begin{aligned} J_p &= \frac{1}{2}\Delta\Sigma + L_q + J_g \\ &= \frac{1}{2}\bar{\psi}\gamma^+\gamma_5\psi - i\bar{\psi}\gamma^+ r\times D\psi \\ &\quad + r\times(E\times B), \end{aligned} \tag{25}$$

where D is the covariant derivative. In 2008, Chen et al. revived the idea to separate the physical degrees from the gauge potential [76, 77]. With this approach, many more decomposition versions were proposed. Then it was observed by Stoilov [78] and further discussed by Lorcé [79, 80] that the separation procedure introduced a so-call Stuekelberg symmetry which copies the structure of the gauge group but acts on fields in a different way. Therefore, the approach by Chen et al. can be viewed as the gauge-invariant extension with Stuekelberg symmetry fixing procedure. Then, all kinds of decompositions are classified into the canonical version, such as Jaffe-Manohar's, and the kinetic (or mechanical) version, such as Ji's. Both of them are in principle measurable without breaking the gauge invariance.

[2]Its value from a recent leading twist NNLO analysis is $0.33 \pm 0.011(\text{theo.}) \pm 0.025(\text{exp.}) \pm 0.028(\text{evol.})$ [67].

4.2 Three-Dimensional Parton Distributions

The general framework to describe the partonic structures of the proton is the generalized transverse momentum dependent parton distributions (GTMDs) [81, 82]. They are related to the Wigner distributions [83, 84] via a transverse Fourier transformation. As the most general one-parton information is contained in the GTMDs, one may obtain the quark orbital angular momentum from the GTMD via the relation:

$$L_q = -\int dx d^2\mathbf{k}_\perp \frac{\mathbf{k}_\perp^2}{M^2} F_{1,4}^q(x, \mathbf{k}_\perp, \mathbf{\Delta}_\perp = 0), \tag{26}$$

where x is the longitudinal momentum fraction, $\mathbf{k}_\perp$ is quark intrinsic transverse momentum, and $\mathbf{\Delta}_\perp$ is the transferred transverse momentum, which is the Fourier conjugate of quark intrinsic transverse coordinate $\mathbf{b}_\perp$. The $F_{1,4}$ depends on the choice of the gauge link that connects the field operators at different positions. A straight path gauge link relates $F_{1,4}$ to the kinetic quark orbital angular momentum, and a light-cone staple-like path gauge link relates it to the canonical one [79, 80]. With a Fourier transformation, one can obtain the relations to the Wigner distribution $\rho_{\text{LU}}(x, \mathbf{k}_\perp, \mathbf{b}_\perp)$ [85]. Unfortunately, neither the GTMD nor the Wigner distribution is currently measurable in experiment.

As illustrated in Fig. 4, one can obtain the generalized parton distributions (GPDs) by integrating the GTMDs over the transverse momentum $\mathbf{k}_\perp$. They can be viewed as the generalization of the PDFs and the form factors. On the other hand, one can obtain the transverse momentum dependent parton distributions (TMDs) by setting the transferred momentum $\mathbf{\Delta}_\perp$ to zero or equivalently integrating the Wigner distributions over the transverse coordinate $\mathbf{b}_\perp$. They

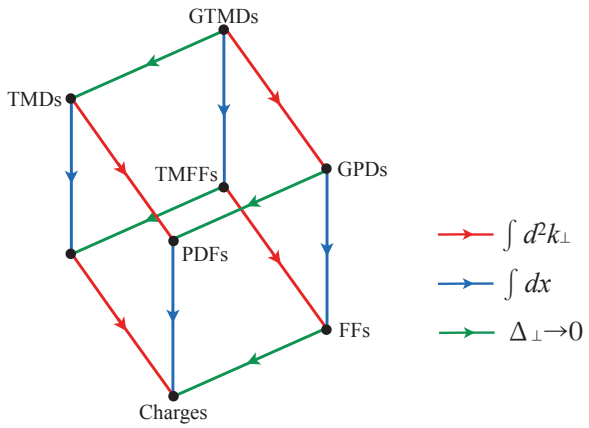

Fig. 4: Parton distribution family.

will reduce to PDFs when the transverse momentum is integrated.

Both the GPDs and the TMDs are three-dimensional parton distributions. They have a much richer spin dependence than PDFs, and are related to quark orbital angular momentum with some model dependent or model independent relations. One well-known relation is the total quark angular momentum with the gravitational (or generalized) form factors, which are the second moments of the GPDs [75] that can be measured through the deeply virtual Compton scatterings [86]. Together with the measurement of quark helicity distributions, one may obtain the kinetic quark orbital angular momentum via the GPDs:

$$L_q = \int dx[xH^q(x,0,0)+xE^q(x,0,0)-\tilde{H}^q(x,0,0)], \tag{27}$$

though it is questioned by some recent model calculations [87, 88]. With QCD equation of motion, it is also related to a twist-three GPD as [89]

$$L_q = -\int dx\, xG_2^q(x,0,0). \tag{28}$$

On the aspect of TMDs, the pretzelosity TMD $h_{1T}^{\perp}(x,\mathbf{k}_\perp)$ is proposed as a quantity to measure quark orbital angular momentum through

$$L_q = -\int dx d^2\mathbf{k}_\perp \frac{\mathbf{k}_\perp^2}{2M^2} h_{1T}^{\perp q}(x,\mathbf{k}_\perp), \tag{29}$$

which is first observed from spectator model calculations [90] and is proved valid for all spherically symmetric situations [91]. The pretzelosity function is one of eight leading twist TMDs, and it will lead to the single spin asymmetry in the semi-inclusive DIS (SIDIS) processes [92]. This asymmetry has been measured in some experiments by COMPASS [93, 94, 95, 96], HERMES [97] and Jefferson Lab [98]. A most recent extraction of the pretzelosity from the data indicates positive up-quark pretzelosity and negative down-quark pretzelosity [99] but with big errors which allow both positive and negative signs. Future experimental data from JLab 12 [100] will be essential to determine the pretzelosity distributions.

Apart from the pretzelosity TMD, it is also proposed to estimate quark orbital angular momentum from the Sivers function $f_{1T}^{\perp}(x,\mathbf{k}_\perp)$ [101], which is related to the GPD $E(x,\xi,\mathbf{\Delta}_\perp)$ with a lensing function in a model dependent way [102]. The Sivers function, as well as the Boer-Mulders function $h_1^{\perp}(x,\mathbf{k}_\perp)$, is a naively time-reversal odd leading twist TMD [103]. The nonvanishing Sivers function can arise from the final (or initial) state interaction mechanism [104, 105], or more generally from the gauge link. Then, a sign change is predicted for the Sivers functions in the SIDIS process and the Drell-Yan process [106, 107, 108]. Therefore, a precise measurement of the Sivers function, as well as the Boer-Mulders function, is a direct examination of the TMD factorization and QCD. The Drell-Yan program at COMPASS [109] and the SIDIS program at Jefferson Lab [110, 111] will improve our knowledge on these TMDs.

4.3 Tensor Charge and Electric Dipole Moment

The tensor charge associated with a quark flavor in the proton is defined via the matrix element of the tensor current as

$$\langle P,S|\bar{\psi}_q i\sigma^{\mu\nu}\psi_q|P,S\rangle = \delta_T q \bar{u}(P,S) i\sigma^{\mu\nu} u(P,S). \tag{30}$$

It is one fundamental partonic structure of the proton. As shown in Fig. 4, the charges can be obtained by integrating the PDFs over the Bjorken scaling variable x. At the leading twist, the vector charge, axial charge and tensor charge are respectively obtained from the unpolarized parton distribution, helicity distribution and transversity distribution. In the parton model, the vector charge is interpreted as the valence quark number. The axial charge measures the difference of the number of quark and antiquark with helicity parallel to that of the proton and the number of quark and antiquark with helicity antiparallel to that of the proton, while the tensor charge measures the transverse polarized valence quark number induced by the transverse polarization of the proton as

$$\delta_T q = \int dx [h_1^q(x) - h_1^{\bar{q}}(x)]. \tag{31}$$

As mentioned at the beginning of this section, the measurement of the axial charge induced the proton spin puzzle and evoked active studies in this field. Therefore, it deserves the effort to measure the tensor charge, if one intends to unravel the spin structure of the proton. The transversity can be measured through the SIDIS process in the TMD factorization framework and the dihadron production process in the collinear factorization framework [112]. It is also measurable in the Drell-Yan process with at lease one particle transversely polarized [113], but such data are not available yet. In Fig. 5, we plot the tensor charges extracted from current data [114, 115, 116] and calculated from lattice QCD [117, 118, 119]. Although the extractions of the tensor charge are consistent with each other, the value of the u quark tensor charge looks systematically smaller than the ones from the lattice simulation. More precise measurement is required. The future experiments at Jefferson Lab will improve our knowledge on the tensor charge [120, 121, 122]. Especially, the SIDIS experiment [110] in SoLID program, which is designed to operate with a high luminosity and a large acceptance, will provide a far more precise measurement on the transversity distribution, and hence a determination of the tensor charge. The accuracy is expected to be comparable with that of current lattice simulations as shown in Fig. 5.

In addition, the tensor charge is related to the electric dipole moment (EDM) of the proton and the neutron. It is known that the nonzero EDM carried by a spin-1/2 particle is a signal of time-reversal symmetry violation. Assuming the CPT-invariance, such effect can only arise from the CP-violation interaction, which is expected small. Since the existence of an electric monopole charge usually overwhelms the signal from the EDM, it is more natural to measure the EDM of the neutron, which is the simplest spin-1/2 neutral particle. The current upper limit of neutron EDM is $2.9 \times 10^{-26} e\,\mathrm{cm}$ at 90% C.L. [123].

One direct contribution to the neutron EDM is from the quark EDM. The effective interaction is expressed as

$$\mathcal{L}_{\mathrm{eff}} = -\frac{1}{2} d_q \bar{\psi}_q i\sigma^{\mu\nu}\gamma_5 \psi_q F_{\mu\nu}, \tag{32}$$

where d_q is the quark EDM. Then, its contribution to the neutron EDM is

$$d_n = d_u \delta_T u + d_d \delta_T d + d_s \delta_T s. \tag{33}$$

In the standard model, the quark EDM, about $10^{-34} e\,\mathrm{cm}$, is induced by the complex phase in the Cabibbo-Kobayashi-Maskawa (CKM) matrix at three-loop level [124]. A larger quark EDM can arise from the CP-violation interactions beyond the standard model. Therefore, the precise measurement of the tensor charge, together with neutron EDM, will provide stringent constraints on quark EDM, which can be utilized to search for new physics.

5 Summary

Charge, mass and spin are three fundamental properties of a particle, and they are the most general information of our knowledge on a physical object from classical to quantum and from macro to micro. Even for a black hole, charge,

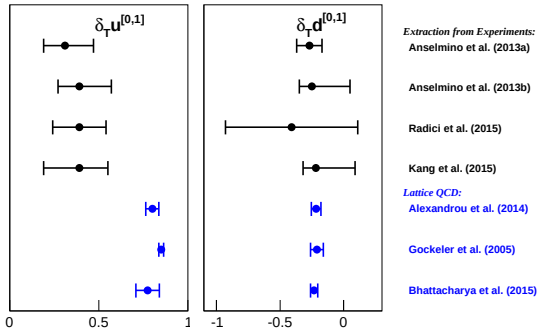

Fig. 5: Tensor charge from experimental data [114, 115, 116] and lattice simulations [117, 118, 119].

mass and spin are the only accessible information [125, 126, 127]. Therefore, one can never say any particle is well understood before its charge, mass and spin are successfully interpreted. The proton, which is the only stable hadron and directly involved into all of four fundamental interactions, has been investigated for a century. However, we still have very poor knowledge on its structure of charge, mass and spin.

In this paper, we discuss the present status and upcoming experiments on all these puzzles: proton charge radius puzzle, proton mass budget and proton spin puzzle. The PRad experiment at Jefferson Lab [30], the μp elastic scattering experiment at PSI [31], the ISR experiment at Mainz [32], and new hydrogen spectroscopy experiments [33] will provide high precision measurements of proton charge radius from different aspects in order to resolve the proton radius puzzle. The near threshold electroproduction of J/ψ experiment in SoLID program at Jefferson Lab will provide a direct measurement on the trace anomaly part of the proton mass through the quarkonium-nucleon low-energy scattering [60]. It will lead to a more precise determination of the proton mass budget. The SIDIS experiment at Jefferson Lab [100] and the Drell-Yan experiment at COMPASS [109] are aiming to unravel the spin structure of the proton. In addition, the precise measurement of the transversity in these experiments will also improve the accuracy of the determination of the tensor charge, which can be utilized to search for new physics together with the measurement of neutron EDM. Therefore, the experiments in the upcoming decade will help to resolve these puzzles and to bring our knowledge on the proton to a new stage.

Acknowledgments

This work is supported in part by U.S. Department of Energy under contract number DE-FG02-03ER41231 and NSF MRI award PHY-1229153. This work is also supported by the National Natural Science Foundation of China under Grant No. 11120101004. We thank K. Allada, J.-P. Chen, D. Dutta, A. Gasparian, N. Gonzalez, M. Khandaker, M. Meziane, Z.-E. Meziani, A. Prokudin for useful discussions.

References

[1] H. Gao, Int. J. of Mod. Phys. E **12**, 1 (2003).

[2] C.E. Hyde-Wright and K. de Jager, Annu. Rev. Nucl. Part. Sci. **54**, 217 (2004).

[3] J. Arrington, C.D. Roberts, J.M. Zanotti, J. Phys. **G34**, S23 (2007).

[4] S.E. Kuhn, J.-P. Chen, E. Leader, Prog. Part. Nucl. Phys. **63**, 1 (2009).

[5] R. Pohl *et al.*, Nature **466**, 213 (2010).

[6] A. Antognini *et al.*, Science **339**, 417 (2013).

[7] J.C. Bernauer *et al.*, Phys. Rev. Lett. **105**, 242001 (2010).

[8] J.C. Bernauer *et al.*, Phys. Rev. C **90**, 015206 (2014).

[9] X. Zhan *et al.*, Phys. Lett. B **705**, 59 (2011).

[10] J. Arrington and I. Sick, J. Phys. Chem. Ref. Data **44**, 031204 (2015).

[11] J. Arrington, arXiv:1506.00873 [nucl-ex].

[12] P.J. Mohr, D.B. Newell, and B.N. Taylor, arXiv:1507.07956 [atom-ph].

[13] I. Sick, Phys. Lett. B **576**, 62 (2003).

[14] M.C. Birse and J.A. McGovern *et al.*, Eur. Phys. J. A **48**, 120 (2012).

[15] G.A. Miller, Phys. Lett. B **718**, 1078 (2013).

[16] J.M. Alarcón, V. Lensky, and V. Pascalutsa, Eur. Phys. J. C **74**, 2852 (2014).

[17] U.D. Jentschura, Ann. Phys. **326**, 500 (2011).

[18] A. Antognini *et al.*, Ann. Phys. **331**, 127 (2013).

[19] V. Barger *et al.*, Phys. Rev. Lett. **106**, 153001 (2011).

[20] C. Carlson and B. Rislow, Phys. Rev. D **86**, 035013 (2012).

[21] B. Batell, D. Mckeen and M. Pospelov Phys. Rev. Lett. **107**, 011803 (2011).

[22] R. Onofrio, Europhys. Lett. **104**, 20002 (2013).

[23] I.T. Lorentz, H.-W. Hammer, Ulf-G. Meißner, Eur. Phys. J. A **48**, 151 (2012).

[24] D. Robson Int. J. Mod. Phys. E **23**, 14500906 (2014).

[25] T.W. Donnelly, D.K. Hasell, and R.G. Milner, arXiv:1505.04723 [nucl-ex].

[26] G. Lee, J. Arrington, and R. Hill Phys. Rev. D **92**, 013013 (2015).

[27] K. Griffioen, C. Carlson, S. Maddox, arXiv:1509.06676 [nucl-ex].

[28] D.W. Higinbotham *et al.*, arXiv:1510.01293 [nucl-ex].

[29] M.O. Distler, T. Walcher and J.C. Bernauer, arXiv:1511.00479 [nucl-ex].

[30] A. Gasparian (PRad Collaboration), EPJ Web Conf. **73**, 07006 (2014).

[31] R. Gilman *et al.*, arXiv:1303.2160 [nucl-ex].

[32] M. Mihovilovic *et al.*, EPJ Web Conf. **72**, 00017 (2014).

[33] A.C. Vutha *et al.*, BAPS.2012.DAMOP.D1.138 (2012).

[34] G. Aad *et al.* (ATLAS Collaboration), Phys. Lett. B **716**, 1 (2012).

[35] S. Chatrchyan *et al.* (CMS Collaboration), Phys. Lett. B **716**, 30 (2012).

[36] I.C. Cloet and C.D. Roberts, Prog. Part. Nucl. Phys. **77**, 1 (2014).

[37] S.J. Brodsky, G.F. de Terámond, H.G. Dosch and J. Erlich, Phys. Rep. **584**, 1 (2015).

[38] S.J. Brodsky, H.C. Pauli and S.S. Pinsky, Phys. Rep. **301**, 299 (1998).

[39] X. Ji, Phys. Rev. Lett. **74**, 1071 (1995).

[40] X. Ji, Phys. Rev. D **52**, 271 (1995).

[41] L.A. Harland-Lang, A.D. Martin, P. Motylinski and R.S. Thorne, Eur. Phys. J. C **75**, 204 (2015).

[42] M. Hoferichter, J. Ruiz de Elvira, B. Kubis and U.G. Meißner, Phys. Rev. Lett. **115**, 092301 (2015).

[43] R.D. Young and A.W. Thomas, Phys. Rev. D **81**, 014503 (2010).

[44] S. Deldar, H. Lookzadeh and S.M.H. Nejad, Phys. Rev. D **85**, 054501 (2012).

[45] S. Durr *et al.*, Phys. Rev. D **85**, 014509 (2012).

[46] R. Horsley *et al.* (QCDSF-UKQCD Collaboration), Phys. Rev. D **85**, 034506 (2012).

[47] G.S. Bali *et al.* (QCDSF Collaboration), Phys. Rev. D **85**, 054502 (2012).

[48] W. Freeman *et al.* (MILC Collaboration), Phys. Rev. D **88**, 054503 (2013).

[49] H. Ohki *et al.* (JLQCD Collaboration), Phys. Rev. D **87**, 034509 (2013).

[50] M. Engelhardt, Phys. Rev. D **86**, 114510 (2012).

[51] P. Junnarkar and A. Walker-Loud, Phys. Rev. D **87**, 114510 (2013).

[52] M. Gong *et al.* (XQCD Collaboration), Phys. Rev. D **88**, 014503 (2013).

[53] M.F.M. Lutz, R. Bavontaweepanya, C. Kobdaj and K. Schwarz, Phys. Rev. D **90**, 054505 (2014).

[54] Y.-B. Yang, A. Alexandru, T. Draper, J. Liang and K.-F. Liu, arXiv:1511.09089 [hep-lat].

[55] P. Gubler and K. Ohtani, Phys. Rev. D **90**, 094002 (2014).

[56] K.A. Olive *et al.* (Particle Data Group), Chin. Phys. C **38**, 090001 (2014).

[57] D. Kharzeev, Proc. Int. Sch. Phys. Fermi **130**, 105 (1996).

[58] D. Kharzeev, H. Satz, A. Syamtomov and G. Zinovjev, Eur. Phys. J. C **9**, 459 (1999).

[59] A. Deur, S.J. Brodsky and G.F. de Terámond, Phys. Lett. B **750**, 528 (2015).

[60] E12-12-006, https://www.jlab.org/exp_prog/proposals/12/PR12-12-006.pdf.

[61] S.J. Brodsky, I.A. Schmidt and G.F. de Terámond, Phys. Rev. Lett. **64**, 1011 (1990).

[62] S.J. Brodsky, E. Chudakov, P. Hoyer and J.M. Laget, Phys. Lett. B **498**, 23 (2001).

[63] J. Ashman *et al.* (European Muon Collaboration), Phys. Lett. B **206**, 364 (1988).

[64] J. Ashman *et al.* (European Muon Collaboration), Nucl. Phys. B **328**, 1 (1989).

[65] E.S. Ageev *et al.* (COMPASS Collaboration), Phys. Lett. B **612**, 154 (2005).

[66] V.Y. Alexakhin *et al.* (COMPASS Collaboration), Phys. Lett. B **647**, 8 (2007).

[67] A. Airapetian *et al.* (HERMES Collaboration), Phys. Rev. D **75**, 012007 (2007).

[68] E.P. Wigner, Annals Math. **40**, 149 (1939) [Nucl. Phys. Proc. Suppl. **6**, 9 (1989)].

[69] B.-Q. Ma, J. Phys. G **17**, L53 (1991).

[70] B.-Q. Ma and Q.-R. Zhang, Z. Phys. C **58**, 479 (1993).

[71] D. de Florian, R. Sassot, M. Stratmann and W. Vogelsang, Phys. Rev. Lett. **113**, 012001 (2014).

[72] E. Leader and C. Lorcé, Phys. Rep. **541**, 163 (2014).

[73] M. Wakamatsu, Int. J. Mod. Phys. A **29**, 1430012 (2014).

[74] R.L. Jaffe and A. Manohar, Nucl. Phys. B **337**, 509 (1990).

[75] X. Ji, Phys. Rev. Lett. **78**, 610 (1997).

[76] X.-S. Chen, X.-F. Lu, W.-M. Sun, F. Wang and T. Goldman, Phys. Rev. Lett. **100**, 232002 (2008).

[77] X.-S. Chen, W.-M. Sun, X.-F. Lu, F. Wang and T. Goldman, Phys. Rev. Lett. **103**, 062001 (2009).

[78] M.N. Stoilov, Bulg. J. Phys. **41**, 251 (2014).

[79] C. Lorcé, Phys. Rev. D **87**, no. 3, 034031 (2013).

[80] C. Lorcé, Phys. Lett. B **719**, 185 (2013).

[81] S. Meissner, A. Metz and M. Schlegel, JHEP **0908**, 056 (2009).

[82] C. Lorcé and B. Pasquini, JHEP **1309**, 138 (2013).

[83] X. Ji, Phys. Rev. Lett. **91**, 062001 (2003).

[84] C. Lorcé and B. Pasquini, Phys. Rev. D **84**, 014015 (2011).

[85] C. Lorcé, B. Pasquini, X. Xiong and F. Yuan, Phys. Rev. D **85**, 114006 (2012).

[86] X. Ji, Phys. Rev. D **55**, 7114 (1997).

[87] T. Liu and B.-Q. Ma, Phys. Lett. B **741**, 256 (2014).

[88] T. Liu and B.-Q. Ma, Phys. Rev. D **91**, 017501 (2015).

[89] D.V. Kiptily and M.V. Polyakov, Eur. Phys. J. C **37**, 105 (2004).

[90] J. She, J. Zhu and B.-Q. Ma, Phys. Rev. D **79**, 054008 (2009).

[91] C. Lorcé and B. Pasquini, Phys. Lett. B **710**, 486 (2012).

[92] A. Bacchetta, M. Diehl, K. Goeke, A. Metz, P.J. Mulders and M. Schlegel, JHEP **0702**, 093 (2007).

[93] B. Parsamyan (COMPASS Collaboration), Eur. Phys. J. ST **162**, 89 (2008).

[94] B. Parsamyan, J. Phys. Conf. Ser. **295**, 012046 (2011).

[95] B. Parsamyan (COMPASS Collaboration), Phys. Part. Nucl. **45**, 158 (2014).

[96] B. Parsamyan, PoS DIS **2013**, 231 (2013).

[97] G. Schnell (HERMES Collaboration), PoS DIS **2010**, 247 (2010).

[98] Y. Zhang *et al.* (Jefferson Lab Hall A Collaboration), Phys. Rev. C **90**, 055209 (2014).

[99] C. Lefky and A. Prokudin, Phys. Rev. D **91**, 034010 (2015).

[100] J. Dudek *et al.*, Eur. Phys. J. A **48**, 187 (2012).

[101] A. Bacchetta and M. Radici, Phys. Rev. Lett. **107**, 212001 (2011).

[102] M. Burkardt, Nucl. Phys. A **735**, 185 (2004).

[103] J.C. Collins, Nucl. Phys. B **396**, 161 (1993).

[104] S.J. Brodsky, D.S. Hwang and I. Schmidt, Phys. Lett. B **530**, 99 (2002).

[105] S.J. Brodsky, D.S. Hwang and I. Schmidt, Nucl. Phys. B **642**, 344 (2002).

[106] J.C. Collins, Phys. Lett. B **536**, 43 (2002).

[107] J.C. Collins and A. Metz, Phys. Rev. Lett. **93**, 252001 (2004). k

[108] D. Boer, P.J. Mulders and F. Pijlman, Nucl. Phys. B **667**, 201 (2003).

[109] F. Gautheron *et al.* (COMPASS Collaboration), CERN-SPSC-2010-014.

[110] E12-10-006, http://hallaweb.jlab.org/collab/PAC/PAC34/PR-09-014-transversity.pdf.

[111] E12-11-108, https://www.jlab.org/exp_prog/proposals/11/PR12-11-108.pdf.

[112] A. Bacchetta, A. Courtoy and M. Radici, Phys. Rev. Lett. **107**, 012001 (2011).

[113] V. Barone, A. Drago and P.G. Ratcliffe, Phys. Rept. **359**, 1 (2002).

[114] M. Anselmino, M. Boglione, U. D'Alesio, S. Melis, F. Murgia and A. Prokudin, Phys. Rev. D **87**, 094019 (2013).

[115] M. Radici, A. Courtoy, A. Bacchetta and M. Guagnelli, JHEP **1505**, 123 (2015).

[116] Z.-B. Kang, A. Prokudin, P. Sun and F. Yuan, arXiv:1505.05589 [hep-ph].

[117] C. Alexandrou, M. Constantinou, K. Jansen, G. Koutsou and H. Panagopoulos, PoS LATTICE **2013**, 294 (2014).

[118] M. Gockeler *et al.* (QCDSF and UKQCD Collaborations), Phys. Lett. B **627**, 113 (2005).

[119] T. Bhattacharya, V. Cirigliano, R. Gupta, H.-W. Lin and B. Yoon, Phys. Rev. Lett. **115**, 212002 (2015).

[120] H. Gao *et al.*, Eur. Phys. J. Plus **126**, 2 (2011).

[121] H. Avakian, EPJ Web Conf. **66**, 01001 (2014).

[122] J.-P. Chen *et al.* (SoLID Collaboration), arXiv:1409.7741 [nucl-ex].

[123] C.A. Baker *et al.*, Phys. Rev. Lett. **97**, 131801 (2006).

[124] A. Czarnecki and B. Krause, Phys. Rev. Lett. **78**, 4339 (1997).

[125] W. Israel, Phys. Rev. **164**, 1776 (1967).

[126] B. Carter, Phys. Rev. Lett. **26**, 331 (1971).

[127] D.C. Robinson, Phys. Rev. Lett. **34**, 905 (1975).